

mirror symmetry of  $A = 3$  nuclei could be exploited through simultaneous measurements of the inclusive structure functions for  ${}^3\text{He}$  and  ${}^3\text{H}$  to provide an independent measurement of this ratio. Both methods are designed to largely eliminate the nuclear corrections, thereby permitting the neutron-to-proton ratio (and thus the  $d/u$  ratio) to be extracted with unprecedented precision.

The measurement of structure functions over the large kinematic range made available with the 12 GeV Upgrade will also allow moments, or  $x$ -weighted integrals, of both spin-polarized and unpolarized structure functions to be determined accurately. Certain moments of polarized structure functions, for example, are related to the color-electric and magnetic polarizabilities of the nucleon, which characterize the response of the gluon fields to the nucleon’s polarization. These moments are also directly calculable from first principles using lattice QCD simulations, and will thus provide critical tests of QCD itself.

### The Generalized Parton Distributions as Accessed via Deeply Exclusive Reactions

The Generalized Parton Distributions tell us a great deal more about the physics of partons than do the individual Feynman distributions and the form factors. For example, one can determine the quark angular momentum distribution from the GPDs. The total quark contribution to the spin of the nucleon can be determined by the following sum rule [Ji97]:

$$J^q = \frac{1}{2}\Delta\Sigma - L^q = \frac{1}{2} \int_{-1}^1 x dx [H^q(x, \xi, 0) + E^q(x, \xi, 0)] \quad (1)$$

The quark spin part contribution,  $\Delta\Sigma$ , has been measured for the last decade through polarized deep-inelastic scattering. Therefore, an experimental determination of  $J^q$  allows a measurement of the quark orbital angular momentum, a quantity hard to determine otherwise.

One of the striking findings that has emerged from the theoretical study of the GPDs is that they can be measured through a new class of “hard” exclusive processes: Deeply Virtual Compton Scattering (DVCS) and Deeply Virtual Meson Production (DVMP). Both of these reactions are a subset of deep inelastic scattering in which specific exclusive final states are measured. As shown schematically in Fig. 12, in DVCS the electron knocks a quark out of the proton by exchanging a deeply virtual (massive) photon. The quark then emits a high energy photon and is put back into the proton. In DVMP a  $q\bar{q}$  pair is created, and a quark is returned into the proton while the  $\bar{q}$  picks up a quark from the vacuum to form a meson. At sufficiently high energy and virtuality of the exchanged photon (Bjorken regime) these hard processes can be described by perturbative QCD, and the cross sections can be used to extract the “soft” information of the nucleon described by the GPDs.

At energies and momentum transfers currently available at JLab, photons are produced not only via DVCS but also (even more copiously) via the electromagnetic Bethe-Heitler (BH) process. The two processes interfere, and the BH term, which is completely determined by the well known elastic form factors, “boosts” the much smaller and unknown DVCS term, which is determined by the GPDs, to comfortably measurable levels. During the past two years DVCS has become an

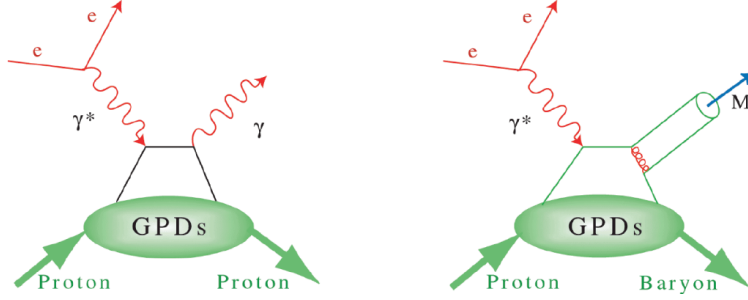


Figure 12: The “handbag” diagrams for deeply virtual Compton scattering (left), and for deeply virtual meson production (right). Four GPDs describe the “soft” proton structure part. They depend on the longitudinal quark momentum fraction  $x$ , and two more variables: the longitudinal momentum imbalance of the quark before and after the interaction,  $\xi$ , and the momentum transferred to the proton,  $t$ .

established tool of GPD studies with experimental results from CLAS [St01] at JLab and from the HERA experiments H1 [Ad01], ZEUS [Sa01], and HERMES [Ai01]. These data are well described in a consistent GPD analysis in leading order (LO) and next to leading order (NLO) QCD [Fr01], supporting the applicability of the GPD formalism to exclusive photon production even at relatively low  $Q^2$ . However, with the present maximum beam energy of 6 GeV these experiments are limited to a modest fraction of the interesting range of the kinematic variables. An example of the much broader kinematic coverage in  $Q^2$ ,  $x_B$ , and  $t$  for the DVCS program, achievable with the equipment proposed for the 12 GeV upgrade, is shown in Fig.13. Similar coverage can be achieved for the GPD program in meson production.

Polarized beam asymmetry measurements allow the extraction of GPDs or linear combinations of GPDs at fixed kinematics  $x = \xi$ , while cross section measurements determine integrals of GPDs at fixed values of  $\xi$  and  $t$ . Different combinations of GPDs can be measured using polarized targets. DVCS off unpolarized protons cannot separate contributions from different quark flavors or separate the spin-dependent from the spin-independent GPDs. DVMP is another tool to study GPDs; it can make these separations. Vector meson production, (*e.g.*  $\rho$  and  $\omega$ ) permit the isolation of the spin-independent GPDs and separate  $u$  and  $d$  quark contributions, while pseudoscalar meson production (*e.g.*  $\pi^0$ ,  $\eta$ ) accesses the spin-dependent GPDs.

A full program to extract GPDs from measurements requires coverage of a large kinematic range in  $\xi$ ,  $t$ , and  $Q^2$ , and measurement of several final states together with the use of polarized beam and polarized targets with longitudinal and transverse polarization. The 12 GeV upgrade of the electron accelerator and of the equipment required for the GPD program will provide the kinematic coverage needed for a broad program of DVCS and DVMP. Doubling the energy of the current accelerator in conjunction with the very high luminosity will allow access to the highest  $Q^2$  and  $\xi$  values of any facility worldwide. These unprecedented capabilities will allow a comprehensive program of DVCS and DVMP to be carried out.

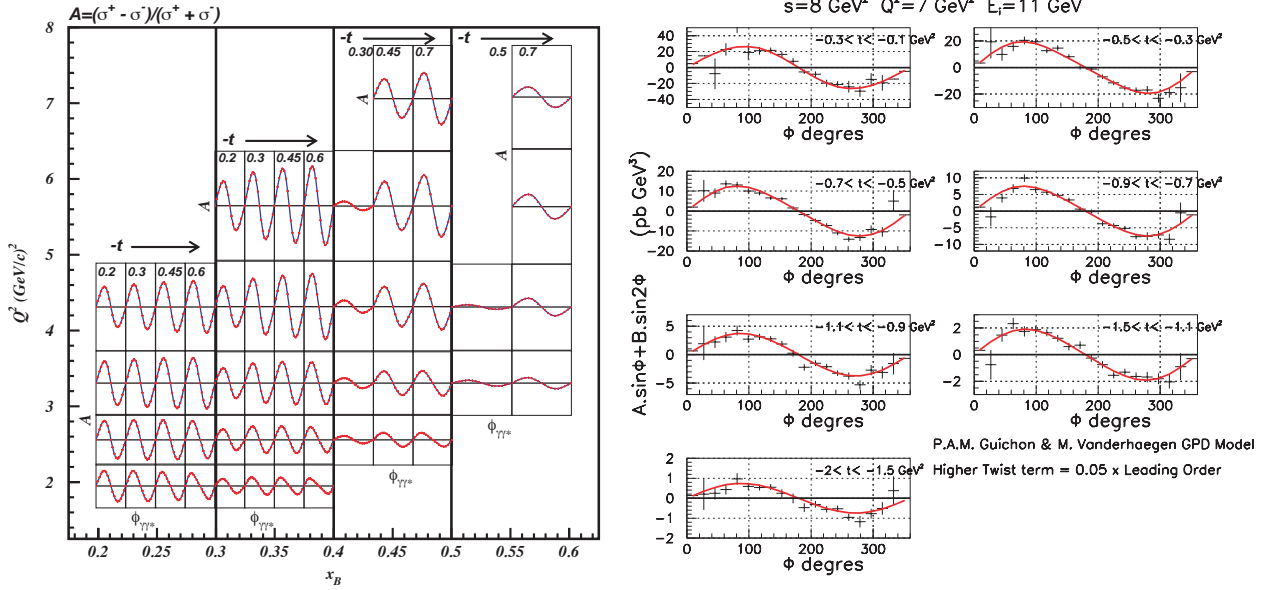


Figure 13: Beam spin asymmetry for  $\vec{e}p \rightarrow ep\gamma$ . Projected data and error bars for kinematic coverage of DVCS/BH asymmetry measurements. The left panel shows the lower  $t$  portion of azimuthal asymmetries that can be accessed simultaneously. The curves represent a specific model for the GPDs. The right panel shows projected data at the highest  $Q^2$  for cross section differences. In kinematics, where the DVCS cross section is large, absolute cross section measurements will be possible giving access to moments of different combinations of GPDs.

The results of this program, together with results at smaller  $\xi$  from other laboratories, will form the basis for the ultimate extraction of the GPDs. Recently, it has been realized that the GPDs provide the quantum phase-space (Wigner) distributions of the quarks and gluons [Ji03c, Be03a]. A phase-space function represents a correlated momentum and coordinate distribution and is much more powerful than the momentum or coordinate space distribution alone. While quantum phase-space distributions have been widely used in many different areas, they have not been studied systematically for subatomic systems. Using a GPD parameterization fitted to measured form factors and parton distributions, Belitsky *et al.* [Be03a] obtained the phase-space charge distributions shown in Fig. 14. These quark images are 3D pictures of the quark charge distribution for selected Feynman momentum  $x$ , corresponding to the full distribution seen through Feynman momentum (“color”) filters. At very small  $x$ , the quarks spread out in the direction of the momentum, going as far as  $1/x$ . At large  $x$ , the quantum nature of the distribution becomes very clear and the image looks like a diffraction pattern. At intermediate  $x$  where the valence quarks dominate, the image is like what we normally think of the proton.

An alternate visualization of nucleon structure, showing the quark-flavor distribution and the spin-flavor polarization for the  $u$  and  $d$  quarks in unpolarized and transversely polarized protons, is shown in Figure 15. These distributions were constructed by Burkardt [Bu02] from models for the GPDs  $H(x, \xi = 0, b_\perp)$  and  $E(x, \xi = 0, b_\perp)$ . Even five years ago it was unimaginable that we would ever be able to obtain such detailed and revealing images of proton structure.

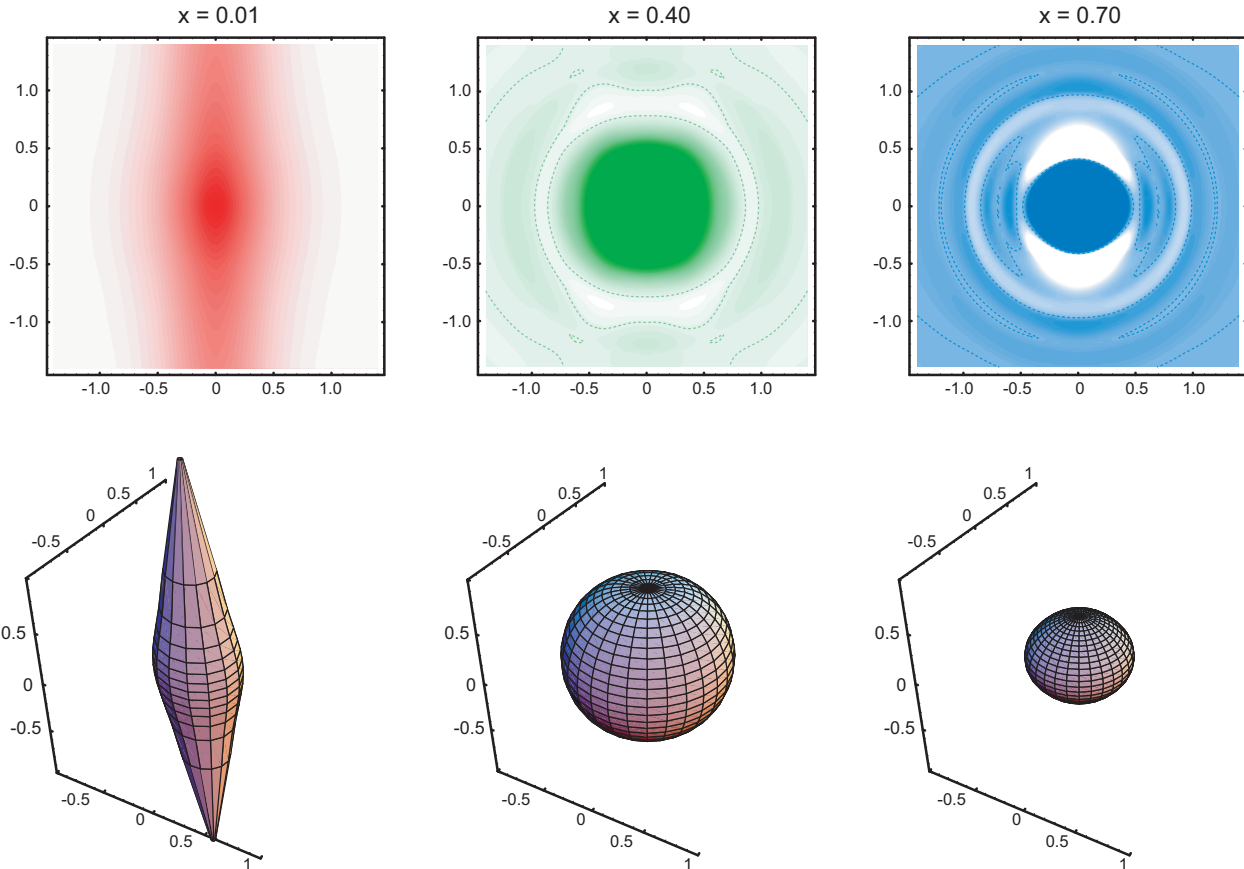


Figure 14: A model  $u$ -quark phase space charge distribution in 3D coordinate space for three Feynman momentum fractions:  $x= 0.01, 0.40,$  and  $0.70$ . In the upper pictures the vertical axis corresponds to the longitudinal direction selected by the virtual photon that defined  $x$ . The pictures are rotationally symmetric in the transverse direction, which is shown here as the horizontal axis. The lower set of figures show the shape of a constant density contour for the corresponding distribution above.

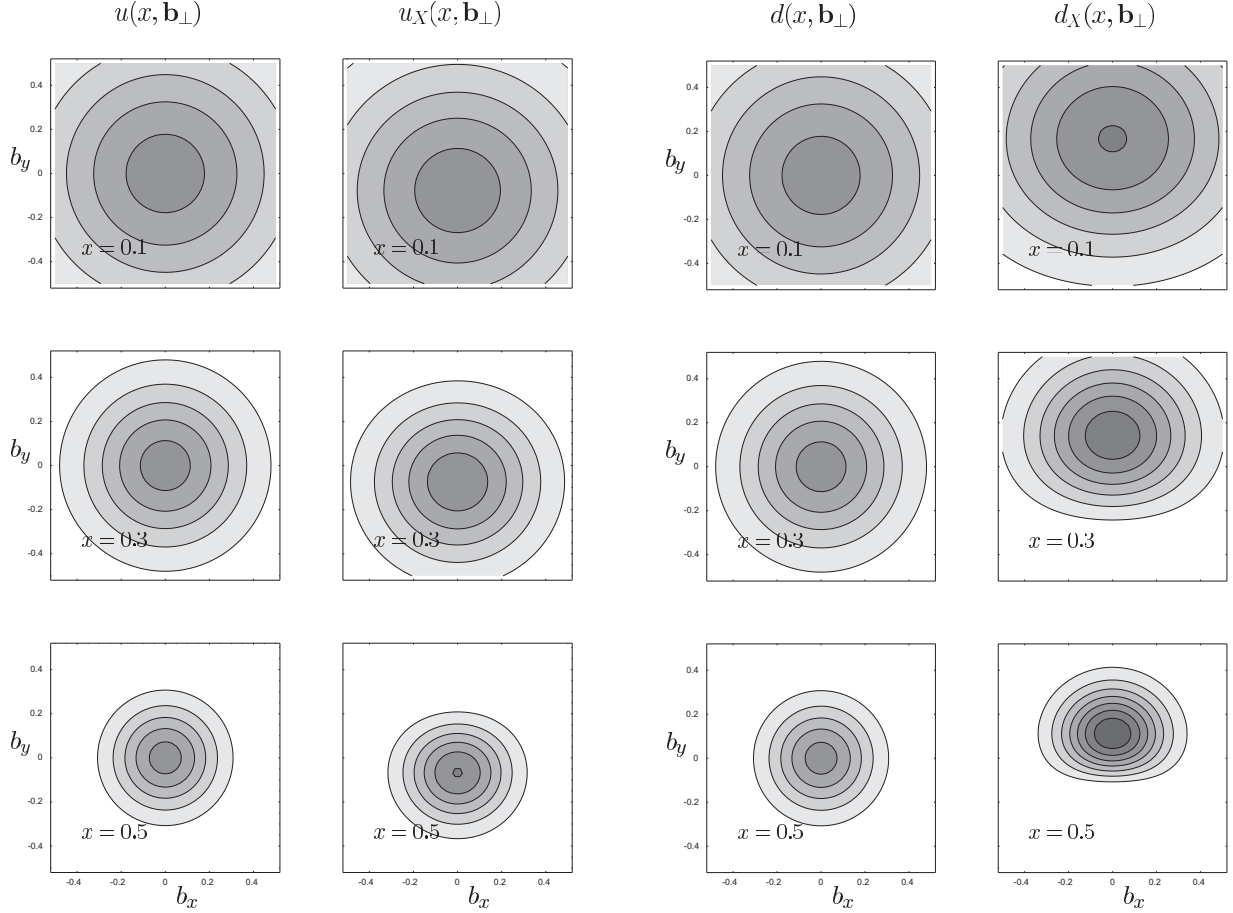


Figure 15: The quark spatial and spin distributions in the transverse plane from model calculations. The left panels show the  $u$  quark longitudinal momentum and helicity distributions in transverse impact parameter space. The panels on the right show the corresponding images for the  $d$  quarks in the proton. A strong correlation between the transverse size and the longitudinal momentum is evident. For small quark momentum fractions  $x$ , the proton has a large transverse size, and it becomes very dense at large  $x$ . The right columns in each panel show the quark spin distributions in a transversely polarized proton.  $u$  and  $d$  quarks exhibit a strong and opposite spatial asymmetry. Quarks in a transversely polarized protons have a strong spin-flavor polarization, especially at high  $x$ . The general features of these plots are model independent.